CHEMISTRY OF MATERIALS
Article

Chem. Mater. **2011,** *23,* 771–777 771
DOI:10.1021/cm1018585

Star-Shaped Oligotriarylamines with Planarized Triphenylamine Core: Solution-Processable, High-T_g Hole-Injecting and Hole-Transporting Materials for Organic Light-Emitting Devices†

Zuoquan Jiang,‡ Tengling Ye,§ Chuluo Yang,*,‡ Dezhi Yang,§ Minrong Zhu,‡ Cheng Zhong,‡ Jingui Qin,‡ and Dongge Ma*,§

‡*Department of Chemistry, Hubei Key Lab on Organic and Polymeric Optoelectronic Materials, Wuhan University, Wuhan 430072, People's Republic of China, and* §*State Key Laboratory of Polymer Physics and Chemistry, Changchun Institute of Applied Chemistry, Chinese Academy of Sciences, Changchun 130022, People's Republic of China*

Received July 3, 2010. Revised Manuscript Received November 7, 2010

Two novel star-shaped oligotriarylamines with planar triphenylamine core and peripheral triarylamine groups, namely FATPA-T and FATPA-Cz, were synthesized by Suzuki cross-coupling reaction. The molecular design imparts the materials with the following features: (i) excellent thermal stabilities with quite high glass transition temperatures (237 °C for FATPA-T and 272 °C for FATPA-Cz); (ii) good solution-processability; (iii) good hole mobility, efficient hole injection, and electron-blocking functions. Furthermore, their optoelectronic properties can be modulated by the peripheral triarylamine groups. For example, FATPA-T with triphenylamine peripheries shows the significantly red-shifted absorption and emission, as well as the small band gap as compared to FATPA-Cz with carbazole peripheries. Double-layer Alq_3-emitting OLEDs using FATPA-T or FATPA-Cz as hole-transport layer by spin-coating method were fabricated, and the FATPA-Cz-based devices show greatly improved performance as compared to standard NPB-based device by vacuum-evaporation of NPB. The optimized three-layer Alq_3-emitting OLEDs by using FATPA-Cz and NPB as double hole-transport layers exhibit the maximum current efficiency of 6.83 cd/A, which is the highest for the Alq_3-based green emission under the similar device structures. The advantages of solution-processablity and very high T_g make the star-shaped oligotriarylamines ideal substitutes for conventional arylamines as hole-inject and hole-transport materials.

1. Introduction

Triarylamine derivatives have been widely used as hole-transporting materials in thin layer optoelectronic devices such as organic light-emitting diodes (OLEDs), organic photovoltaic cells (OPV), and organic field-effect transistors (OFETs).[1] However, the monomeric molecules do not exhibit a high hole-transport efficiency due to their easy crystallinity and/or low thermal stability.[2] In many OLEDs, the hole-transporting materials are the weakest link, with regard to thermal stability. For example, the glass-transition temperature (T_g) for aluminum tris(8-hydroxyquinoline) (Alq_3), a common electron-transporting material, is 175 °C, whereas those for the standard hole-transporting materials, such as 1, 4-bis(1-naphthylphenyl)amino)biphenyl (NPB) and *N*,*N*′-bis(3-methylphenyl)-1,1′-biphenyl-4, 4′-diamine (TPD), are 96 and 65 °C, respectively.[3] The expansion of the hole-transporting layer (HTL) in a thermally stressed OLED can cause the device degradation. This effect can be reduced using HTL materials with high T_g.[4] To improve the amorphous nature, various oligotriarylamines with linear, star-shaped, branched or dendritic structures have been developed.[5] Shirota et al. have reported several families of high T_g star-shaped oligotriarylamines with different cores (benzene, triphenylbenzene or triphenylamine); furthermore, in these systems the extended conjugation can result in a low oxidation potential, in consequence a low barrier for hole injection from anode.[6] The most efficient conjugation

† Accepted as part of the "Special Issue on π-Functional Materials".

*Corresponding author. E-mail: clyang@whu.edu.cn (C.Y.); mdg1014@ciac.jl.cn (D.M.).

(1) (a) Tang, C. W.; Van Slyke, S. A. *Appl. Phys. Lett.* **1987**, *51*, 9131. (b) Thelakkat, M. *Macromol. Mater. Eng.* **2002**, *287*, 442. (c) Wu, J.; Baumagarten, M.; Debije, M. G.; Warman, J. M.; Müllen, K. *Angew. Chem., Int. Ed.* **2004**, *43*, 5331. (d) Shirota, Y.; Kageyama, H. *Chem. Rev.* **2007**, *107*, 953.

(2) (a) Burroughes, J. H.; Bradley, D. D. C.; Brown, A. R.; Marks, R. N.; Mackay, K.; Friend, R. H.; Burn, P. L.; Holmes, A. B. *Nature* **1990**, *347*, 539. (b) Friend, R. H.; Gymer, R. W.; Holmes, A. B.; Burroughes, J. H.; Marks, R. N.; Taliani, C.; Bradley, D. D. C.; Dos Santos, D. A.; Bredas, J. L; Logdlund, M.; Salaneck, W. R. *Nature* **1999**, *397*, 121.

(3) Naito, K.; Miura, A. *J. Phys. Chem.* **1993**, *97*, 6240.

(4) O'Brien, D. F.; Burrows, P. E.; Forrest, S. R.; Koene, B. E.; Loy, D. E.; Thompson, M. E. *Adv. Mater.* **1998**, *10*, 1108.

(5) (a) Shirota, Y. *J. Mater. Chem.* **2000**, *10*, 1. (b) Satoh, N.; Cho, J. S.; Higuchi, M.; Yamamoto, K. *J. Am. Chem. Soc.* **2003**, *125*, 8104. (c) Shirota, Y. *J. Mater. Chem.* **2005**, *15*, 75. (d) Li, Z. A.; Liu, Y.; Yu, G.; Wen, Y.; Guo, Y.; Ji, L.; Qin, J.; Li, Z. *Adv. Funct. Mater.* **2009**, *19*, 2677. (e) Lee, T. W.; Kim, H. S.; Cho, M. J.; Kim, K. H.; Choi, D. H. *Chem. Lett.* **2008**, *37*, 952. (f) Paul, G. K.; Mwaura, J.; Argun, A. A.; Taranekar, P.; Reynolds, J. R. *Macromolecules* **2006**, *39*, 7789.

(6) (a) Ishikawa, W.; Inada, H.; Nakano, H.; Shirota, Y. *Chem. Lett.* **1991**, 1731. (b) Shirota, Y.; Kobata, T.; Noma, N. *Chem. Lett.* **1989**, 1145. (c) Inada, H.; Shirota, Y. *J. Mater. Chem.* **1993**, *3*, 319. (d) Okumoto, K.; Ohara, T.; Noda, T.; Shirota, Y. *Synth. Met.* **2001**, *121*, 1655.

Published on Web 11/23/2010

was observed in the 4,4′,4″-tris(diphenylamino)triphenylamine (TDATA) series in which the nitrogen atoms are connected through a phenylene group via paralinkages.[6b]

The layer-by-layer evaporation has been proven to be a successful technique in the fabrication of OLEDs; however, it is also restricted by high cost, time-consuming and low process yield. Convenient solution processing such as spin coating or inkjet printing has been desired as an easy preparation of devices with low cost and large area.[7] For example, PVK (polyvinylcarbazole), has been widely used as solution-processable hole-transporting material in OLEDs.[8] However, as compared to vacuum-evaporated materials, the solution-processable, small-molecule-based hole-transporting materials have little reported to date.

Hellwinkel et al. initially reported a series of bridged triarylamine compounds.[9] Recently, the bridged triarylamine derivatives attracted attentions in organic optoelectronics.[10] We reported a new fully diarylmethene-bridged triphenylamine (FATPA), which has an almost planar triphenylamine (TPA) skeleton and exhibits excellent thermal and morphological stability.[11] In this paper, we report the synthesis and the structures of two novel star-shape arylamines with the planarized FATPA as molecular core and triphenylamine or carbazole as peripheral group. The new star-shaped arylamines are applicable in the OLEDs as morphologically stable hole-transport materials having a good hole mobility, efficient hole injection, and electron-blocking functions. Moreover, the novel materials are solution-processable. All the merits make them very attractive hole-transporting materials in OLEDs.

2. Experimental Section

General Information. ^{1}H NMR and ^{13}C NMR spectra were measured on Varian Unity 300 MHz spectrometer using $CDCl_3$ as solvent. Elemental analyses of carbon, hydrogen, and nitrogen were performed on a Vario EL-III microanalyzer. EI-MS spectra were recorded with a VJ-ZAB-3F-Mass spectrometer. MALDI-TOF mass spectrometric measurement was performed on Bruker Biflex III MALDI TOF instrument. Differential scanning calorimetry (DSC) was performed on a NETZSCH DSC 200 PC unit at a heating rate of 10 °C min^{-1} from 30 to 600 °C under argon. Thermogravimetric analysis (TGA) was undertaken with a NETZSCH STA 449C instrument. The thermal stability of the samples under a nitrogen atmosphere was determined by measuring their weight loss while heating at a rate of 10 °C min^{-1} from 25 to 600 °C. UV−vis absorption spectra were recorded on Shimadzu UV-2550 spectrophotometer. PL spectra were recorded on Hitachi F-4500 fluorescence spectrophotometer. Cyclic voltammetric measurements were carried out on a computer-controlled EG&G potentiostat/galvanostat model 283 using tetrabutylammonium hexafluorophosphate (0.1 M) in freshly distilled CH_2Cl_2 solution as supporting electrolyte and conventional three-electrode cell with a Pt button working electrode of 2 mm diameter, a platinum-wire counter electrode, and a Ag/AgCl reference electrode with ferrocenium−ferrocene (Fc^+/Fc) as the internal standard.

Synthesis of FATPA-Br. To a solution of FATPA (1.0 g, 1.22 mmol) in 20 mL of chloroform was added NBS (0.68 g, 3.82 mmol) at 0 °C. The mixture was stirred for 12 h at room temperature, and then filtered. The filtrate was washed with water three times, and the organic layers were dried with anhydrous sodium sulfate. After removal of organic solvent, the resulting solid was recrystallized from ethanol to give a white solid (Yield: 95%). ^{1}H NMR (300 MHz, $CDCl_3$, δ): 6.91 (s, 6H), 6.86 (d, J = 8.1 Hz, 12 H), 6.55 (d, J = 8.1 Hz, 12 H), 2.30 (s, 18 H); ^{13}C NMR (75 MHz, $CDCl_3$, δ): 141.81, 136.13, 134.26, 130.77, 130.70, 130.01, 128.70, 116.10, 55.29, 21.12. Anal. Calcd. for $C_{63}H_{48}Br_3N$ (%): C, 71.47; H, 4.57; N, 1.32. Found: C, 71.23; H, 4.40; N, 1.35; MALDI-TOF-MS: m/z 1059.2 (M^+).

Synthesis of FATPA-T. A mixture of FATPA-Br (0.60 g, 0.57 mmol), *N*-(4-(4,4,5,5-tetramethyl-1,3,2-dioxaborolan-2-yl)phenyl)-*N*-phenylbenzenamine (0.84 g, 2.26 mmol), $Pd(PPh_3)_4$ (40 mg, 2% mmol) and sodium carbonate (1.81 g, 17.1 mmol) in 40 mL of toluene and 9 mL of distilled water was stirred at 90 °C for 36 h under argon. The mixture was extracted with toluene, and the organic layers were washed with brine, dried over anhydrous sodium sulfate. The crude product was purified by column chromatography on silica gel using 3:1 (v/v) petroleum/chloroform as the eluent to afford a yellow solid (Yield: 81%). ^{1}H NMR (300 MHz, $CDCl_3$, δ): 7.18−7.15 (m, 18 H), 7.05−6.91 (m, 30 H), 6.78 (d, J = 7.2 Hz, 12 H), 6.65 (d, J = 7.2 Hz, 12 H), 2.21 (s, 18 H); ^{13}C NMR (75 MHz, $CDCl_3$, δ): 165.17, 165.13, 149.00, 147.91, 144.45, 136.60, 135.70, 135.08, 131.47, 130.56, 129.52, 128.19, 127.03, 125.64, 125.25, 124.13, 56.93, 22.32. Anal. Calcd. for $C_{117}H_{90}N_4$ (%): C, 90.54; H, 5.85; N, 3.61. Found: C, 91.01; H, 6.16; N, 3.36. MALDI-TOF-MS: m/z 1551.5 (M^+).

Synthesis of FATPA-Cz. A mixture of FATPA-Br (0.60 g, 0.57 mmol), 9-(4-*tert*-butylphenyl)-3-(4,4,5,5-tetramethyl-1,3,2-dioxaborolan-2-yl)-9H-carbazole (0.28 g, 2.26 mmol), $Pd(PPh_3)_4$ (40 mg, 2% mmol) and sodium carbonate (1.81 g, 17.1 mmol) in 40 mL of toluene and 9 mL of distilled water was stirred at 90 °C for 36 h under argon. The mixture was extracted with toluene, and the organic layers were washed with brine, dried over anhydrous sodium sulfate. The crude product was purified by column chromatography on silica gel using 3:1 (v/v) petroleum/chloroform as the eluent to afford a yellow solid (Yield: 73%). ^{1}H NMR (300 MHz, $CDCl_3$, δ): 7.99 (d, J = 8.1 Hz, 3H), 7.52 (d, J = 8.1 Hz, 9H), 7.37−7.26 (m, 24H), 6.83−6.76 (m, 27H), 2.25 (s, 18H), 1.34 (s, 27H); ^{13}C NMR (75 MHz, $CDCl_3$, δ): 150.40, 143.28, 141.37, 140.09, 135.39, 135.19, 134.85, 134.18, 132.94, 130.24, 129.24, 128.15, 126.97, 126.67, 126.61, 126.54, 126.45, 125.85, 124.99, 123.47, 123.26, 120.17, 119.68, 117.95, 109.92, 109.87, 55.69, 30.88, 29.67, 20.94. Anal. Calcd. for $C_{129}H_{108}N_4$ (%): C, 90.38; H, 6.35; N, 3.27. Found: C, 90.71; H, 6.63; N, 2.94. MALDI-TOF-MS: m/z 1712.9 (M^+).

Device Fabrication and Measurements. The ITO-coated glass substrates were cleaned with special detergent and deionized water. After cleaning, the substrates were baked at 120 °C for 20 min followed by O_2 plasma treatment. FATPA-T or FATPA-Cz were

(7) (a) Zhou, G.; Wong, W. Y.; Yao, B.; Xie, Z.; Wang, L. *Angew. Chem., Int. Ed.* **2007**, *46*, 1149. (b) Ge, Z.; Hayakawa, T.; Ando, S.; Ueda, M.; Akiike, T.; Miyamoto, H.; Kajita, T.; Kakimoto, M. *Chem. Mater.* **2008**, *20*, 2532.
(8) Zhang, K.; Chen, Z.; Yang, C.; Zhang, X.; Tao, Y.; Duan, L.; Chen, L.; Zhu, L.; Qin, J.; Cao, Y. *J. Mater. Chem.* **2007**, *17*, 3451.
(9) (a) Bamberger, S.; Hellwinkel, D.; Neugebauer, F. A. *Chem. Ber.* **1975**, *108*, 2416. (b) Hellwinkel, D.; Melan, M. *Chem. Ber.* **1974**, *107*, 616. (c) Hellwinkel, D.; Schmidt, W. *Chem. Ber.* **1980**, *113*, 358.
(10) (a) Takizawa, H. Jpn. Kokai Tokkyo Koho 11339868, Dec 10, 1999. (b) Aoki, K.; Yamazaki, H.; Mishima, M.; Togashi, H.; Sakuma, T. Jpn. Kokai Tokkyo Koho 05107784, Apr 30, 1993. (c) Parham, A.; Vestweber, H.; Heun, S.; Heil, H.; Stoessel, P.; Fortte, R. German Patent DE 102005043163, Mar 15, 2007. (d) Parham, A.; Heun, S.; Vestweber, H.; Stoessel, P.; Heil, H.; Fortte, R. U.S. Patent 20090295275, Dec 3, 2009. (e) Fang, Z.; Teo, T.-L.; Cai, L.; Lai, Y.-H.; Samoc, A.; Samoc, M. *Org. Lett.* **2009**, *11*, 1. (f) Fang, Z.; Zhang, X.; Yee, H.; Liu, B. *Chem. Commun.* **2009**, 920.
(11) Jiang, Z.; Chen, Y.; Yang, C.; Cao, Y.; Tao, Y.; Qin, J.; Ma, D. *Org. Lett.* **2009**, *11*, 1503.

spin-coated from the solution in chlorobenzene onto the precleaned ITO substrates. After baking at 120 °C for 30 min, the emitting layer of Alq_3 was deposited by thermal evaporation at a base pressure $< 1 \times 10^{-4}$ Pa. At last, a 1 nm thick layer of LiF and a 100 nm thick film Al were thermally deposited as a cathode under vacuum. If needed, NPB was also deposited by thermal evaporation in the same condition. The thickness of the films deposited by thermal evaporation was monitored by the crystal thickness meter and the thickness of spin-coated films was measured by the terrace detector. The active area of the device are 16 mm^2, determined by the cross breadth between the cathode and the ITO. The EL spectra were measured by the JY SPEX CCD3000 spectra. Steady current−luminance−voltage was measured by Keithley 2400 with silicon photodiode. All tests were performed under air atmosphere and at room temperature.

The samples for the TOF measurement were prepared by vacuum deposition using the structure: glass/Ag (30 nm)/HTL (1.1 μm for FATPA-Cz and 1.3 μm for FATPA-T/Al (150 nm). Optical excitation of the carrier packet was achieved by illumination through the Ag electrode using an intense short duration (5−6 ns) light pulse from a frequency-tripled (355 nm) Nd:YAG laser. The transient current was measured across the load resistor using Agilent 54825A Infinium Digital Oscilloscope.

3. Results and Discussion

The synthesis of the star-shaped arylamines, namely FATPA-T and FATPA-Cz, is outlined in Scheme 1. The intermediate 3Br-FATPA was prepared by the bromination of FATPA with NBS in a high yield of 95%. FATPA-T and FATPA-Cz were synthesized by the Suzuki cross-coupling reactions of 3Br-FATPA with 4-triphenylamine pinacol borate or 3-(9-(4-*t*-butyl-phenyl)-9*H*-carbazole) pinacol borate in good yields of 70−80%. Their chemical structures were fully characterized by ^{1}H NMR, ^{13}C NMR, mass spectrometry, and elemental analysis (see the Experimental Section).

The excellent thermal stability of the compounds is indicated by their high decomposition temperatures (T_d, corresponding to 5% weight loss) of 511 °C for FATPA-T and 506 °C for FATPA-Cz in the thermogravimetric analysis (TGA). Distinct glass transition temperatures (T_g) were observed at 237 °C for FATPA-T and 272 °C for FATPA-Cz from the differential scanning calorimetry (DSC), which are much higher than the parent core FATPA (178 °C). To our knowledge, these values are among the highest T_g for hole-transporting materials to date.[12] The bulky star-shaped molecular configuration and the aryl peripheries on the rigid FATPA core could cause entanglement in the amorphous state and hinder recrystallization, which is highly desirable to improve the efficiency and lifetime of OLEDs, especially for high-temperature applications of devices.[13]

Figure 1 shows the absorption spectra of the compounds in toluene and the PL spectra of the compounds in toluene solution and film state, and the photophysical data are summarized in Table 1. Both compounds show almost no absorption beyond 400 nm. The high optical transparency to visible light allows the passage of light emitted from the device to ensure a high light collecting efficiency. The energy gaps are evaluated from the onset of optical absorption of thin films to be 2.88 and 3.02 eV for FATPA-T and FATPA-Cz, respectively. FATPA-T shows the significantly red-shifted absorption and emission, as well as the small band gap as compared to FATPA-Cz, which could be attributed to its larger conjugation than that of FATPA-Cz (Table 1).

The oxidative electrochemical behavior of the compounds was examined by cyclic voltammetry (CV; see Figure 2). FATPA-T and FATPA-Cz show four and three well-defined stepwise-oxidation waves, respectively. Furthermore, the two compounds all exhibit the first reversible oxidation process around 0.29 V (vs Fc^+/Fc). Considering that the identical FATPA core of the two molecules, we assigned the first wave to the oxidation of the central triphenylamino core. Further multistep oxidations occur at the terminal triarylamine units.[14] Their ionization potential (IP) values estimated from $E_{1/2}$ (half-wave potential) of the oxidation are −5.03 and −5.05 eV with regard to the energy level of ferrocene (4.8 eV below vacuum), which are significantly higher than that of central core FATPA (−5.22 eV),[11] hence there must be some delocalization of the charge onto one or more arms of extended structures. The IPs of the two new compounds are close to that of ITO (−4.70 eV), which implies that they could serve as efficient hole-injection materials. The electron affinity (EA) values are deduced from IP values and energy gaps to be −2.15 eV for FATPA-T and −2.04 eV for FATPA-Cz, which suggests that they could also act as efficient electron-blocking materials. The estimate of EA is a gross approximation that does not take the exciton binding energy into account.

We initially fabricated the electroluminescent devices with a simple configuration (Structure I): ITO/HTL (50 nm)/Alq_3 (40 nm)/LiF (1 nm)/Al (100 nm). In these devices, FATPA-T or FATPA-Cz was processed by spin-coating method to serve as hole-transport layer (HTL), and Alq_3 was used as both emissive and electron-transport layer (EML and ETL). A reference device using NPB as HTL by vacuum vapor deposition under the identical configuration was also fabricated for comparison. All the devices show the exclusive green emission originating from Alq_3, indicating no exciplex formation at the interface of HTL/EML.

Figure 3 shows the current−voltage−luminance ($J-V-L$) characteristics and current efficiency vs. current density curves of the three devices. The current densities and luminances of the devices with FATPA-T or NPB as HTL are very similar, while those of the device with FATPA-Cz as HTL are markedly low under the same driving voltage. The device based on FATPA-T and FATPA-Cz exhibit a maximum current efficiency ($\eta_{c\,max}$) of 3.39 and 4.41 cd/A

(12) (a) Chen, J. P.; Tanabe, H.; Li, X. C.; Thoms, T.; Okamura, Y.; Ueno, K. *Synth. Met.* **2003**, *132*, 173. (b) Tong, Q. X.; Lai, S. L.; Chan, M. Y.; Lai, K. H.; Tang, J. X.; Kwong, H. L.; Lee, C. S.; Lee, S. T. *Chem. Mater.* **2007**, *19*, 5851. (c) Jiang, Z.; Liu, Z.; Yang, C.; Zhong, C.; Qin, J.; Yu, G.; Liu, Y. *Adv. Funct. Mater.* **2009**, *19*, 3987.

(13) Loy, D. E.; Koene, B. E.; Thompson, M. E. *Adv.Funct. Mater.* **2002**, *12*, 245.

(14) Chou, M. Y.; Leung, M. K.; Su, Y. O.; Chiang, C. L.; Lin, C. C.; Liu, J. H.; Kuo, C. K.; Mou, C. Y. *Chem. Mater.* **2004**, *16*, 654.

Scheme 1. Synthesis of FATPA-T and FATPA-Cz

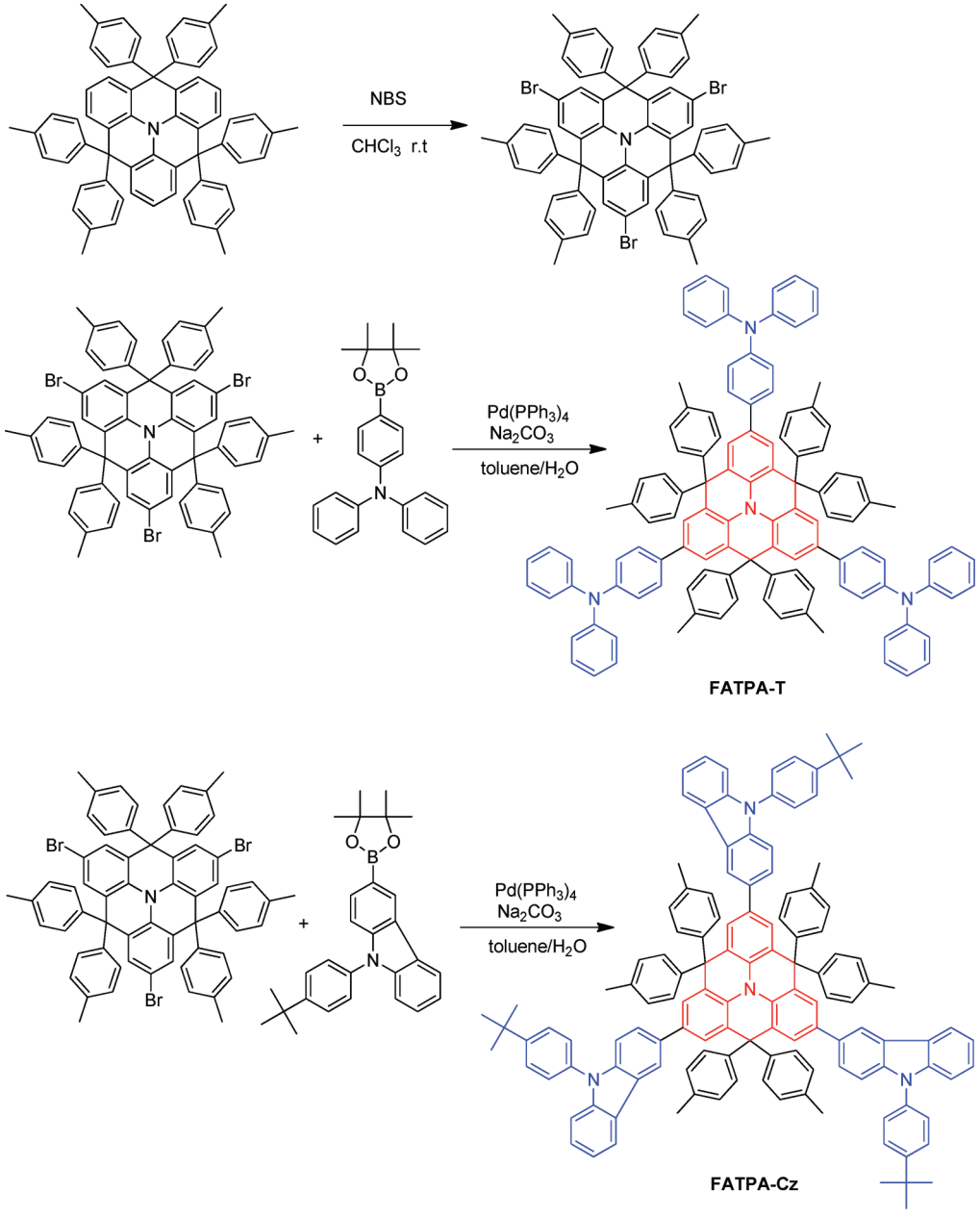

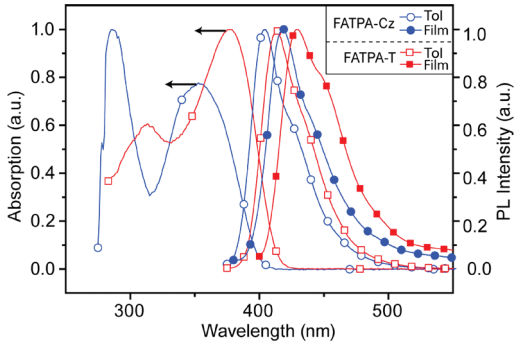

Figure 1. Normalized absorption in toluene and emission spectra in toluene solution and film.

(Table 2), respectively, which are comparable or significantly higher as compared to the NPB-based device (3.14 cd/A). It is worthy to mention that the high efficiencies of the device were achieved by using wet technique to fabricate the hole-transporting layer, which means a more simple process and low cost in comparison with the vacuum vapor deposition for NPB.

To gain insight into the device performances with different HTL, we measured the hole mobilities of the star-shaped arylamines by the time-of-flight (TOF) transient photocurrent technique at room temperature. Both compounds exhibit nondispersive hole-transport characteristics as indicated by the TOF transients. The field-dependence of mobilities determined from the TOF transients (Figure 4) follows the nearly universal Poole-Frenkel relationship.[15] The hole mobilities of 3.1×10^{-4} $cm^2 V^{-1} s^{-1}$ for FATPA-Cz and 6.5×10^{-4} $cm^2 V^{-1} s^{-1}$ for FATPA-T at an electric

(15) (a) Bässler, H. *Int. J. Mol. Phys.* **1994**, *8*, 847. (b) Bässler, H. *Philos. Mag. B* **1992**, *65*, 795. (c) Gill, W. D. *J. Appl. Phys.* **1972**, *43*, 5033.

Table 1. Thermal, Electrochemical, and Photophysical Data of the Compounds

	T_d (°C)	T_g (°C)	IP (eV)	EA (eV)	Abs λ^{max} (nm) soln/film	PL λ^{max} (nm) soln/film
FATPA-T	511	237	−5.03 [a]	−2.15 [b]	378 [c]/383 [d]	414 [c]/429 [d]
FATPA-Cz	506	272	−5.05 [a]	−2.04 [b]	344 [c]/357 [d]	404 [c]/419 [d]

[a] Estimated from the half-wave potential. [b] Deduced from the IP and the optical energy gap. [c] Measured in toluene. [d] Measured in film.

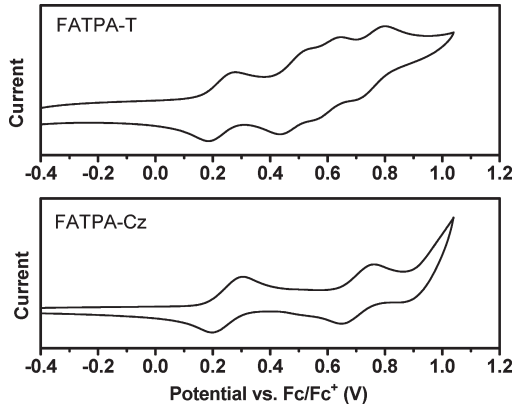

Figure 2. Cyclic voltammogrames of the compounds in CH_2Cl_2 for oxidation.

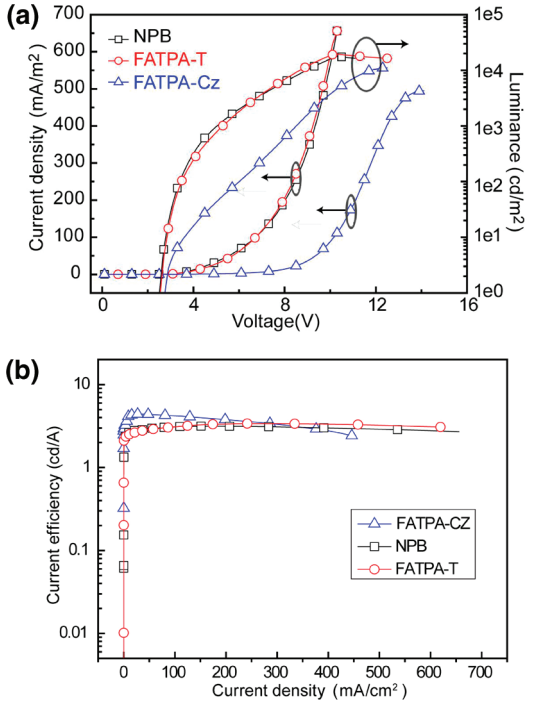

Figure 3. (a) Current density−voltage−luminance characteristics. (b) Current efficiency versus current density curves for device structure I.

field of ca. 1×10^5 V cm^{-1} are lower than that of the typical HTL material NPB (1×10^{-3} cm^2 V^{-1} s^{-1}).[16]

In view of the hole-injection and hole-transport characters of the HTLs, the device performance could be elucidated as follows: (i) Comparing the FATPA-T and NPB, FATPA-T has a substantially lower hole injection barrier from ITO to HTL (~0.35 eV) than NPB (~0.9 eV) (Figure 5), whereas NPB has a significantly lower hole injection barrier from HTL to EML of Alq_3 (0.2 eV) and a higher hole mobility than FATPA-T, the two factors are counteracted to result in the similar current densities and comparable efficiencies for the FATPA-T and NPB-based devices. (ii) Comparing the FATPA-T and FATPA-Cz, both have the same hole-injection barriers, but the hole mobility of FATPA-Cz is smaller than that of FATPA-T, and thus the usage of FATPA-Cz with moderate hole mobility would decrease the hole current, consequently result in more balanced recombination of holes and electrons in the emitting layer. This point could be supported by the lower current density of the FATPA-Cz based device at the given voltage relative to those of FATPA-T or NPB-based devices as discussed above.

Because the hole mobility of FATPA-Cz is still significantly higher than electron mobility of Alq_3,[17] the efficiencies of FATPA-Cz based device were further improved by optimizing the thickness of HTL (90, 115, 135, 150 nm). The best performance is attained in a device with 115 nm thick HTL, and its maximum current efficiency reaches 5.81 cd/A (Figure 6). This indicates that the carrier balance factor is optimal in such a device. For thinner FATPA-Cz layer (50, 90 nm), the holes could be in excess, on the contrary, for thicker FATPA-Cz layer (135, 150 nm), the electrons could be overflow.

Another possible origin of the high device efficiency for FATPA-Cz could be attributed to its efficient electron-blocking function. To confirm the assumption, device structure II: ITO/HTL(115 nm)/Alq_3 (5, 15, 25, or 35 nm)/DCJTB (1 nm)/Alq_3 (35, 25, 15, or 5 nm)/LiF (1 nm)/Al (100 nm), was designed to measure the excitons distribution.[18] In structure II, a thin layer (1 nm) of 4-(dicyanomethylene)-2-(*t*-butyl)-6-methyl-4*H*-pyran (DCJTB) was inserted into the EML at different distances from the interface between the EML and HTL. When excitons were distributed over and decayed in the layer of DCJTB, the corresponding emission spectrum represented a composite of the Alq_3 and DCJTB emissions as shown in Figure 7. The dominant red emission at 5 nm distance away from the HTL layer indicates that the recombination zones of holes and electrons are near the interface of HTL/EML. The small hole mobility relative to electron mobility in Alq3 layer cause the recombination zone to approach the HTL, whereas the efficient electron blocking function of FATPA-Cz make the recombination occur near the interface of HTL/EML.

In terms of the IP values of HTLs, we finally optimized the device structures by using FATPA-Cz and NPB as double hole-transport layers (Structure III): ITO/FATPA-Cz

(16) Lin, L. B.; Young, R. H.; Mason, M. G.; Jenekhe, S. A.; Borsenberger, P. M. *Appl. Phys. Lett.* **1998**, *72*, 864.
(17) Vanslyke, S. A.; Chen, C. H.; Tang, C. W. *Appl. Phys. Lett.* **1996**, *69*, 2160.
(18) Wu, Z.; Wang, L.; Lei, G.; Qiu, Y. *J. Appl. Phys.* **2005**, *97*, 103105.

Table 2. Characteristics of the Electroluminescent Devices

device	HTL	V_{on}[a] (V)	L_{max}[b] (cd m^{-2})	$\eta_{c.max}$[c] (cd A^{-1})	$\eta_{p.max}$[d] (lm W^{1-})	$\eta_{ext.max}$[e] (%)
I	FATPA-T (50 nm)	2.7	11068	3.39	2.35	1.01
I	FATPA-Cz (50 nm)	2.7	19541	4.41	2.63	1.05
I	NPB (50 nm)	2.5	17719	3.14	2.32	1.38
I	FATPA-Cz (90 nm)	2.9	15683	5.21	3.25	1.64
I	FATPA-Cz (115 nm)	3.1	11470	5.81	2.84	1.80
I	FATPA-Cz (135 nm)	3.3	7194	5.43	2.44	1.61
I	FATPA-Cz (150 nm)	3.5	6581	5.43	2.12	1.70
III	FATPA-Cz/NPB (10 nm)	4.9	16405	6.83	2.77	2.07
III	FATPA-Cz/NPB (20 nm)	4.9	16976	6.82	2.77	2.01
III	FATPA-Cz/NPB (30 nm)	4.9	14082	6.19	2.42	1.84
III	FATPA-Cz/NPB (40 nm)	5.1	11966	6.03	1.54	1.85

[a] Turn on voltage. [b] Maximum luminance. [c] Maximum current efficiency. [d] Maximum power efficiency. [e] Maximum external quantum efficiency.

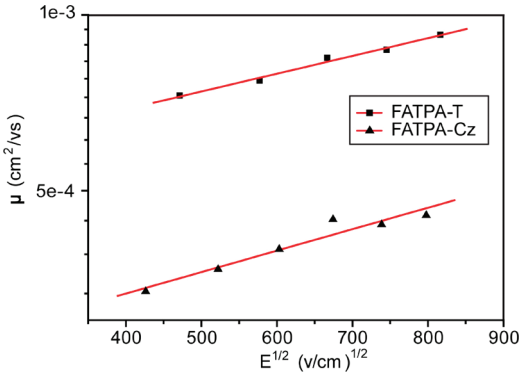

Figure 4. Hole mobilities versus $E^{1/2}$ for films of FATPA-T and FATPA-Cz.

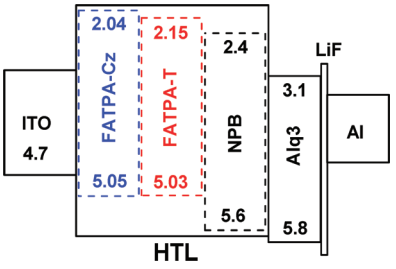

Figure 5. Energy levels of the materials used in the devices.

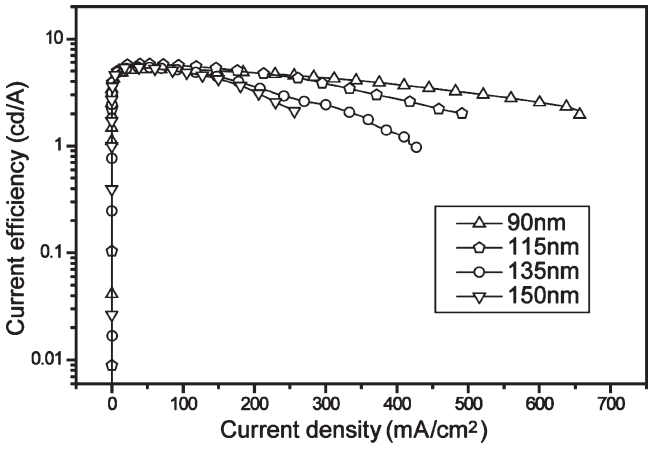

Figure 6. Current efficiency versus current density curves for FATPA-Cz based devices with different HTL thickness.

(115 nm)/NPB (10, 20, 30, or 40 nm)/Alq (40 nm)/LiF (1 nm)/Al (100 nm). Hole carriers are injected in a stepwise process from the anode ITO to the first hole-transport

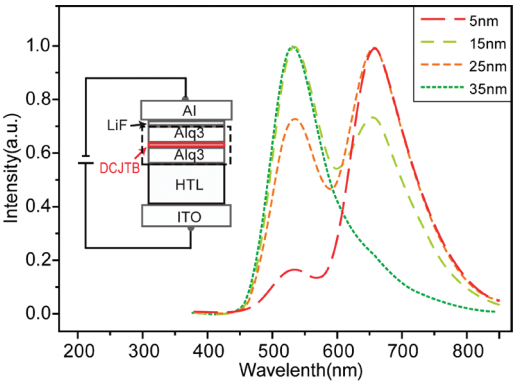

Figure 7. EL spectra for device structure IV.

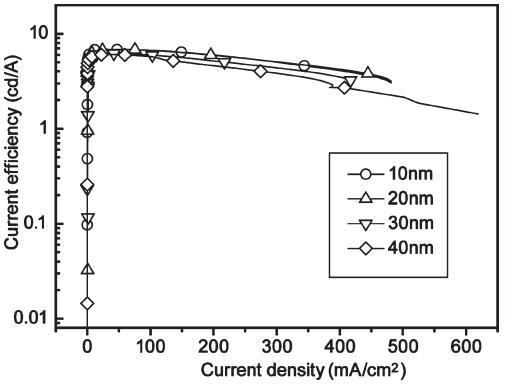

Figure 8. Current efficiency versus current density curves for device structure III.

layer FATPA-Cz, subsequently to the second hole-transport layer NPB, and then to the emitting layer Alq_3. All the devices exhibit high current efficiencies with $\eta_{c\ max}$ in the range of 6.03−6.83 cd/A (Figure 8). The high device efficiencies could be attributed to: (i) The energy barriers for hole injection are lowered by the use of double hole-transport layer structure. The FATPA-Cz here is referred as a hole-injection buffer layer. (ii) When only FATPA-Cz was used as HTL, the recombination zone was located near the interface of HTL/EML since the hole injection barrier from HTL to EML was large. When NPB with faster hole mobility and lower IP was inserted between FATPA-Cz and EML, the hole injection to EML became facile and the recombination zone was extended in the EML and the exciton quenching was efficiently suppressed, in consequence

the device efficiency was further improved.[19] To the best of our knowledge, the maximum current efficiency of 6.83 cd/A obtained at the 10 nm NPB thickness is the highest for the Alq_3-based green emission under the similar device structures until now.[20] Noticeably, the excellent device performance is achieved by using spin-coating method for the hole-transporting layer.

4. Conclusion

In summary, we reported two novel star-shaped oligotriarylamines based on a rigid planar triphenylamine core for the first time. The molecular design imparts the materials with the excellent thermal and morphological stabilities, good solution-processability, and low oxidation potential, which are promising properties for organic optoelectronic devices. Furthermore, their optoelectronic properties can be tuned by the peripheral triarylamine groups. Double-layer Alq_3 emitting OLEDs using FATPA-T or FATPA-Cz as hole-transport layer by spin-coating method were fabricated, and the FATPA-Cz-based device show significantly improved performance as compared to standard NPB-based device by vacuum-evaporation of NPB. Three-layer Alq_3 emitting OLEDs by using FATPA-Cz and NPB as double hole-transport layers exhibit high current efficiencies with $\eta_{c\ max}$ in the range of 6.03−6.83 cd/A, which are the highest for the Alq_3-based green emission under the similar device structures. The advantages of solution-processablity and very high T_g make the star-shaped oligotriarylamines ideal substitutes for conventional arylamines as hole-injection and hole-transport materials.

Acknowledgment. We thank the National Natural Science Foundation of China (Project Nos. 90922020, 50773057), the National Basic Research Program of China (973 Program-2009CB623602, 2009CB930603), the Open Research Fund of State Key Laboratory of Polymer Physics and Chemistry, Changchun Institute of Applied Chemistry, Chinese Academy of Sciences, for financial support.

(19) Tao, Y.; Wang, Q.; Yang, C.; Wang, Q.; Zhang, Z.; Zou, T.; Qin, J.; Ma, D. *Angew. Chem., Int. Ed.* **2008**, *47*, 8104.
(20) Li, J.; Ma, C.; Tang, J.; Lee, C. S.; Lee, S. T. *Chem. Mater.* **2005**, *17*, 615.